Chemistry & Biology
Article

A Systematic Family-wide Investigation Reveals that ~30% of Mammalian PDZ Domains Engage in PDZ-PDZ Interactions

Bryan H. Chang,[1,3] Taranjit S. Gujral,[1,2,3] Ethan S. Karp,[1] Raghida BuKhalid,[1,4] Viara P. Grantcharova,[1,4] and Gavin MacBeath[1,2,*]
[1]Department of Chemistry and Chemical Biology, Harvard University, Cambridge, MA 02138, USA
[2]Department of Systems Biology, Harvard Medical School, Boston, MA 02115, USA
[3]These authors contributed equally to this work
[4]Present address: Merrimack Pharmaceuticals, Inc., Cambridge, MA 02139, USA
*Correspondence: gavin_macbeath@harvard.edu
DOI 10.1016/j.chembiol.2011.06.013

SUMMARY

PDZ domains are independently folded modules that typically mediate protein-protein interactions by binding to the C termini of their target proteins. However, in a few instances, PDZ domains have been reported to dimerize with other PDZ domains. To investigate this noncanonical-binding mode further, we used protein microarrays comprising virtually every mouse PDZ domain to systematically query all possible PDZ-PDZ pairs. We then used fluorescence polarization to retest and quantify interactions and coaffinity purification to test biophysically validated interactions in the context of their full-length proteins. Overall, we discovered 37 PDZ-PDZ interactions involving 46 PDZ domains (~30% of all PDZ domains tested), revealing that dimerization is a more frequently used binding mode than was previously appreciated. This suggests that many PDZ domains evolved to form multiprotein complexes by simultaneously interacting with more than one ligand.

INTRODUCTION

PDZ domains are approximately 90 residues long and were first identified as regions of sequence homology in diverse signaling proteins (Cho et al., 1992; Woods and Bryant, 1993). The name PDZ is derived from the first three proteins in which these domains were found: PSD-95 (a 95 kDa protein involved in signaling in the postsynaptic density); Dlg (the *Drosophila* discs large protein); and ZO1 (the zonula occludens 1 protein involved in maintaining epithelial cell polarity). PDZ domains are found in proteins of diverse function and generally serve as scaffolds for the localization and assembly of multiprotein complexes (Harris and Lim, 2001). They are most often found in combination with other interaction modules and function in a variety of roles that include directing the specificity of receptor tyrosine kinase-mediated signaling (Nourry et al., 2003), establishing and maintaining cell polarity (Bilder, 2001), directing protein trafficking (Sheng and Sala, 2001), and coordinating both presynaptic and postsynaptic-signaling events (Garner et al., 2000).

Most PDZ domain-mediated binding events that have been described to date involve interactions between PDZ domains and the C-terminal tails of their target proteins (Ernst et al., 2009; Songyang et al., 1997). Structural studies have revealed a conserved binding mode in which a peptide ligand docks in an elongated groove between the βB strand and the αB helix of the PDZ domain (Doyle et al., 1996). However, several interactions have been described that do not conform to this canonical-binding mode. For example the PDZ domain of neuronal nitric oxide synthase (nNOS) interacts with the PDZ domain of a1-syntrophin (Hillier et al., 1999) and with the second PDZ domain of PSD95 (Tochio et al., 2000). Both of these interactions are physiologically relevant (Brenman et al., 1996a, 1996b). Structurally, the nNOS PDZ domain has a C-terminal β-hairpin appendage that mimics a C-terminal peptide ligand and docks in the canonical peptide-binding groove of the a1-syntrophin and PSD95 PDZ domains (Hillier et al., 1999; Tochio et al., 2000). PDZ domains have also been found to dimerize in a back-to-back fashion that leaves their peptide-binding grooves available. For example PDZ6 of GRIP1, PDZ1 and PDZ2 of NHERF1, and the PDZ domain of Shank all dimerize in this fashion (Fouassier et al., 2000; Im et al., 2003a, 2003b). In addition the NHERF1 homodimer has been shown to occur in vivo (Maudsley et al., 2000). This alternative binding mode may provide a way for PDZ domains to mediate the assembly of multiprotein complexes by simultaneously interacting with two different targets.

Despite these early findings, very few additional PDZ-PDZ interactions have been reported, and the overall frequency of this binding mode remains unclear. With the goal of discovering additional interactions and establishing the prevalence of this noncanonical-binding mode, we devised a strategy to examine all possible PDZ-PDZ interactions among a large set of mouse PDZ domains. Our approach combines the throughput of protein microarrays and the fidelity of solution-phase fluorescence polarization (FP) with coaffinity purification as a general way to discover and verify novel interactions (Figure 1A). Using this systematic, family-wide approach, we identified a total of 37 PDZ-PDZ interactions involving 46 PDZ domains (~30% of all

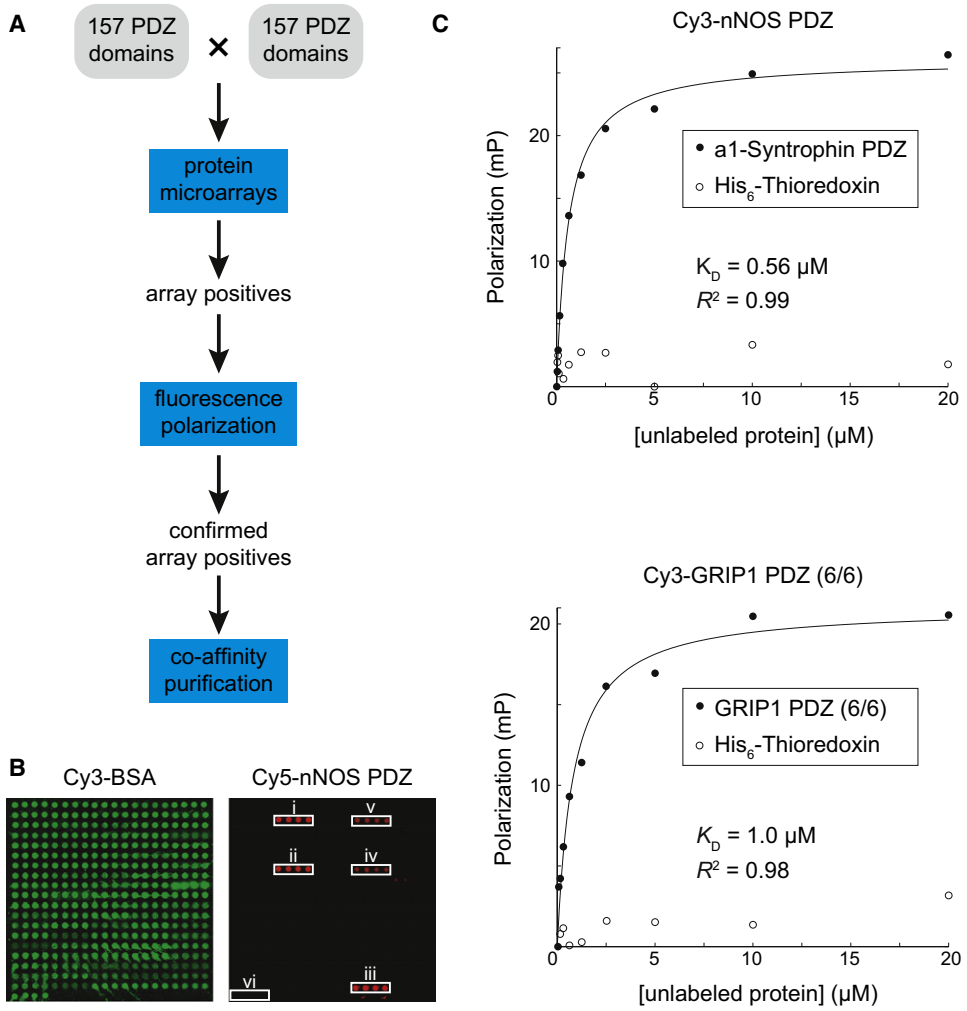

Figure 1. Strategy for the Discovery and Biophysical Validation of PDZ-PDZ Interactions

(A) Strategy to query PDZ-PDZ interactions on a proteome-wide scale. Protein microarrays are used to independently screen all 12,403 possible PDZ-PDZ interactions within a set of 157 mouse PDZ domains. Array-positives are then retested and quantified by FP, thereby removing array false-positives. Finally, PDZ-PDZ biophysically validated PDZ-PDZ interactions are tested for their ability to mediate protein-protein interactions when returned to the context of their full-length parent proteins.

(B) Pilot PDZ domain microarray, probed with Cy5-labeled nNOS PDZ domain. The microarray comprises 96 distinct PDZ domains derived from the mouse proteome, spotted in quadruplicate. The green image (Cy3) shows the location of the PDZ domain spots. The red image (Cy5) shows which PDZ domains are able to interact with nNOS PDZ. In the Cy5 image the white boxes represent interactions of nNOS PDZ domain with the following domains: (i) a1-Syntrophin PDZ; (ii) PSD95 PDZ2; (iii) Chapsyn110 PDZ2; (iv) Rgs12 PDZ; (v) ZO1 PDZ1; and (vi) His_6-Thioredoxin.

(C) Development of an FP assay for detecting and quantifying PDZ-PDZ interactions. The upper plot shows the nNOS PDZ::a1-Syntrophin PDZ heterodimer, and the lower plot shows the GRIP1 PDZ6 homodimer. The filled circles represent PDZ-PDZ interactions, and the open circles represent negative controls (Cy3-PDZ domain mixed with His_6-Thioredoxin). K_D values were obtained by fitting the data to Equation 1.

See also Tables S1 and S2.

PDZ domains tested) and found that many of them mediate stable protein-protein interactions when returned to the context of their full-length proteins. We conclude that PDZ domain dimerization is a more frequently used binding mode than was previously appreciated and submit that many PDZ domains evolved to help assemble multiprotein complexes by simultaneously interacting with more than one ligand. Because PDZ-PDZ interactions appear to be much more selective than PDZ-peptide interactions, it is possible that they contribute more to defining the precise composition of protein complexes than do canonical interactions. Overall, this study uncovered many previously unrecognized protein-protein interactions and serves as a launching point for further investigation of their biological function.

RESULTS AND DISCUSSION

Pilot Experiment Using PDZ Domain Microarrays

To assess the feasibility of using protein microarray technology to systematically screen all possible PDZ-PDZ pairs, we set

out to study interactions between the PDZ domain of nNOS and a representative subset of mouse PDZ domains. We began by assembling a diverse set of 96 mouse PDZ domains (see Table S1 available online), in addition to the nNOS PDZ domain. To abstract individual domains from their full-length proteins, we determined their boundaries by aligning their sequences using ClustalW, a general-purpose multiple-sequence alignment program (http://www.ebi.ac.uk/clustalw/). We then used available structural information to confirm that the boundaries were defined appropriately. The sequence motif GLGF is present in many PDZ domains and forms a carboxylate-binding loop between the first β strand and first α helix. We defined the N termini of our PDZ domain constructs at 15 residues before this motif. Because several studies have shown that additional sequence is required beyond the C termini of PDZ domains to stabilize PDZ-PDZ interactions (Hillier et al., 1999; Maudsley et al., 2000; Utepbergenov et al., 2006; Xu et al., 1998), we included a minimum of 30 additional residues past the predicted end of each PDZ domain in our constructs. When the PDZ domain was located within 30 residues of another domain or occurred at the C terminus of its parent protein, additional sequence was added up to the start of the next domain or to the end of the protein, respectively.

PDZ domains were produced recombinantly in *Escherichia coli*, as previously described (Stiffler et al., 2007). The domains featured N-terminal thioredoxin and His_6 tags and were purified in a single step by immobilized metal affinity chromatography. All of the PDZ domains were verified to be pure, as judged by SDS-polyacrylamide gel electrophoresis, and monomeric, as judged by analytical size exclusion column chromatography (Stiffler et al., 2007).

We have previously reported ways to prepare microarrays of functional proteins in individual wells of 96-well microtiter plates (Stiffler et al., 2006). Briefly, recombinant proteins are microarrayed onto aldehyde-displaying glass substrates that are cut to the size of a microtiter plate. Separate arrays are prepared at the appropriate spacing on each substrate, and the substrates are subsequently attached to the bottom of bottomless microtiter plates using intervening silicone gaskets. Following this procedure the 96 purified PDZ domains were printed in quadruplicate, along with a negative control (His_6-tagged thioredoxin). All domains were mixed with a trace amount (100 nM) of Cy3-labeled bovine serum albumin (BSA) and printed at the same concentration (40 μM). The Cy3-labeled BSA was included to facilitate image analysis. After quenching and blocking the glass surface, the arrays were probed with a single concentration (0.1 μM) of Cy5-labeled nNOS PDZ domain. The arrays were then washed, dried, and scanned for both Cy3 and Cy5 fluorescence (Figure 1B). The Cy3 image was used to identify the locations of all printed PDZ domain spots. Visual inspection of the Cy5 image revealed five specific PDZ-PDZ interactions (Figure 1B).

Confirmation of Pilot Microarray Hits by FP

As with all high-throughput assays, there is an error rate associated with identifying positive interactions. To retest each microarray-positive, we set out to develop a solution-phase assay that is both quantitative and can be used with reasonable throughput. FP is often used to detect and measure the affinity of biomolecular interactions. Although it is best suited for detecting interactions between relatively small molecules and large proteins, it has also been used to detect protein-protein interactions (Jameson and Seifried, 1999; Yan and Marriott, 2003). Because FP is a general assay that can be adapted for large-scale studies, we sought to determine if FP could be used to detect and quantify PDZ-PDZ interactions.

As an initial test, we focused on two well-characterized pairs of PDZ domains that dimerize in structurally distinct ways: the nNOS::a1-syntrophin PDZ domain heterodimer (Brenman et al., 1996a; Hillier et al., 1999); and the GRIP1 PDZ6 homodimer (Im et al., 2003b). In each case a low concentration (25 nM) of Cy3-labeled PDZ domain was mixed with 12 concentrations of its unlabeled partner. For both the nNOS::a1-syntrophin heterodimer and the GRIP1 PDZ6 homodimer, saturation binding was observed (Figure 1C). Under equilibrium conditions, the observed polarization, *FP*, is described by Equation 1:

$$FP = (FP_{max} - FP_0)\frac{K_D + [probe] + [PDZ] - \sqrt{(K_D + [probe] + [PDZ])^2 - 4[probe][PDZ]}}{2[probe]} + FP_0, \quad (1)$$

where FP_{max} is the maximum polarization at saturation, FP_0 is the polarization signal in the absence of PDZ domain, [PDZ] is the total concentration of PDZ domain, [probe] is the total concentration of Cy3-labeled PDZ domain (25 nM), and K_D is the equilibrium dissociation constant. Both data sets fit well to Equation 1 ($R^2 > 0.95$). In addition the observed affinity of the nNOS::a1-syntrophin PDZ domain heterodimer (K_D = 0.56 μM) was consistent with the previously reported value of 0.61 μM (Harris et al., 2001; Harris and Lim, 2001). To verify that the interactions were specific to the PDZ domain portion of the recombinant proteins, His_6-tagged thioredoxin was used as a negative control. As anticipated, no interactions with His_6-thioredoxin were observed (Figure 1C).

Having established this solution-phase assay, we turned our attention to the pilot microarray screen. Of the five PDZ domains that were observed to interact with nNOS PDZ (Figure 1B), three had previously been reported: a1-syntrophin PDZ, PSD95 PDZ2, and Chapsyn110 PDZ2 (Brenman et al., 1996a, 1996b). The other two PDZ domains (ZO-1 PDZ1 and Rgs12 PDZ) were novel. All five of these interactions retested as positive (Figure 2). In addition the observed K_D values for nNOS::a1-syntrophin and nNOS::PSD95 were consistent with previously reported values (Harris et al., 2001; Tochio et al., 2000). Binding to His_6-thioredoxin was not observed in either the microarray or FP assays (Figure 2).

Proteome-wide Investigation of PDZ-PDZ Interactions

To gain a proteome-wide view of PDZ-PDZ interactions, we attempted to clone, express, and purify every PDZ domain

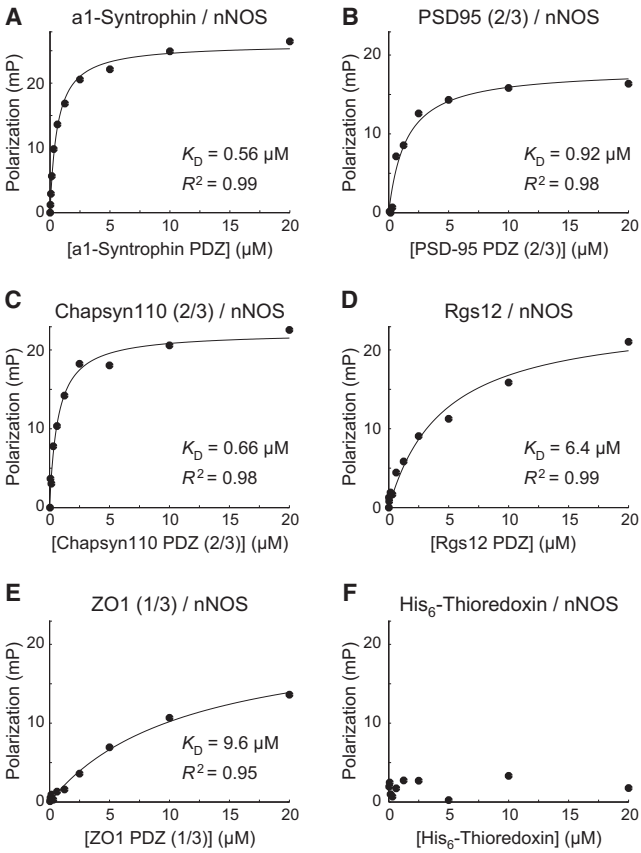

Figure 2. Retesting and Quantifying Array-Positives by FP

Cy3-labeled nNOS PDZ domain was held at a fixed concentration of 25 nM, and unlabeled proteins (PDZ domains or His_6-Thioredoxin) were added at 12 different concentrations, ranging from 20 μM down to 20 nM. K_D values were obtained by fitting the data to Equation 1. Unlabeled proteins were as follows: (A) a1-Syntrophin PDZ; (B) PSD95 PDZ2; (C) Chapsyn110 PDZ2; (D) Rgs12 PDZ; (E) ZO1 PDZ1; and (F) His_6-Thioredoxin. See also Tables S1 and S2.

encoded in the mouse genome. In total we obtained soluble protein of the correct molecular weight for 157 domains (Table S2) (Stiffler et al., 2007). PDZ domain microarrays were prepared by printing the domains, in quadruplicate, in individual wells of 96-well microtiter plates. To assess all 157 × 158 ÷ 2 = 12,403 possible PDZ-PDZ dimers, we labeled each purified PDZ domain individually with Cy5 and probed the PDZ domain microarrays, in triplicate, with 100 nM of each domain (see, for example, Figure 3A). Intensities for each interaction were obtained by taking the mean fluorescence of replicate spots. Z scores (calculated as the number of standard deviations a value is above or below the mean) were generated using the mean intensity of all interactions for each probe (Table S3). Seven Cy5-labeled PDZ domains exhibited excessive background binding on the arrays and so were excluded from subsequent analyses. Because our primary goal was to discover novel interactions, we used a very low Z-score threshold (1.7) to identify hits (Figure 3A; Table S3). This strategy minimizes the number of false-negative interactions but incurs a high false-positive rate. However, we adopted this conservative approach because our secondary assay (FP) was compatible with large-scale studies.

Because the recombinant PDZ domains had been abstracted from their full-length parent proteins, most of them featured non-physiological C termini. It is possible that some of the PDZ-PDZ interactions that we observed on the arrays occurred because one PDZ domain recognized the artificial C terminus of its binding partner. To exclude such artifacts, we evaluated the potential of each C-terminal tail to serve as a ligand for any of the 157 mouse PDZ domains using our previously published PDZ domain-peptide binding data and our predictive models (Chen et al., 2008; Stiffler et al., 2007). PDZ domains with C termini that could potentially serve as ligands were modified: their three C-terminal amino acids were changed to Gly-Gly-Gly. As demonstrated by two independent, large-scale studies of PDZ domains and peptides (Chen et al., 2008; Stiffler et al., 2007), this change precludes their C termini from being recognized by other PDZ domains. These mutant PDZ domains (Figure S1) were used in place of their nonmutated counterparts in all subsequent assays.

To eliminate false-positives in the PDZ domain microarray data set, we retested and quantified all array-positives using our solution-phase FP assay (Table S4). As an additional level of redundancy, each heterodimeric interaction was tested twice, with one or the other domain serving as the Cy3-labeled FP probe. Overall, 628 twelve-point titrations were performed, representing 314 unique PDZ-PDZ interactions. Of these 314 unique interactions, 100 involved at least 1 PDZ domain that had been replaced by a Gly-Gly-Gly C-terminal mutant. Interactions with a K_D <25 μM that fit well to Equation 1 (R^2 > 0.95) were scored as "positive." On the basis of these criteria, 46 of the 157 PDZ domains (~30%) were involved in at least one interaction (Figure 3B and Table 1). Overall, 37 PDZ-PDZ interactions were identified and quantified, 33 of which had not previously been reported (Table 1).

Further Investigation of PDZ-PDZ Interactions by Coaffinity Purification

To determine if the observed PDZ-PDZ interactions can mediate protein-protein interactions in the context of their full-length parent proteins and in a cellular environment, a subset of PDZ-PDZ interaction pairs with K_D <5 μM was chosen and tested using a co-AP assay. Full-length or near full-length open reading frames (ORFs) encoding 15 different proteins were cloned into Gateway-compatible mammalian expression vectors to generate Myc- and HA-tagged proteins (Table S5). The constructs were cotransfected into HEK293T cells, the cells were lysed, and soluble protein complexes were immunoprecipitated using an anti-Myc antibody. HEK293T cells singly transfected with HA-tagged expression constructs served as negative controls.

In total we tested 11 PDZ-PDZ interactions (2 known and 9 novel) using co-AP assays. As anticipated, the two previously reported PDZ-PDZ-mediated interactions—nNOS::Chapsyn110 (Brenman et al., 1996b) and GRIP1::GRIP1 (Im et al., 2003b)—were detected (Figure 4A). Heterodimerization of GRIP1 with GRIP2 and homodimerization of GRIP2 were also observed (Figure 4B). However, it should be noted that although these latter two protein-protein interactions had previously been reported (Srivastava et al., 1998), no specific PDZ-PDZ interactions had been assigned to them (GRIP1 and GRIP2 both contain more than one PDZ domain). More importantly, the

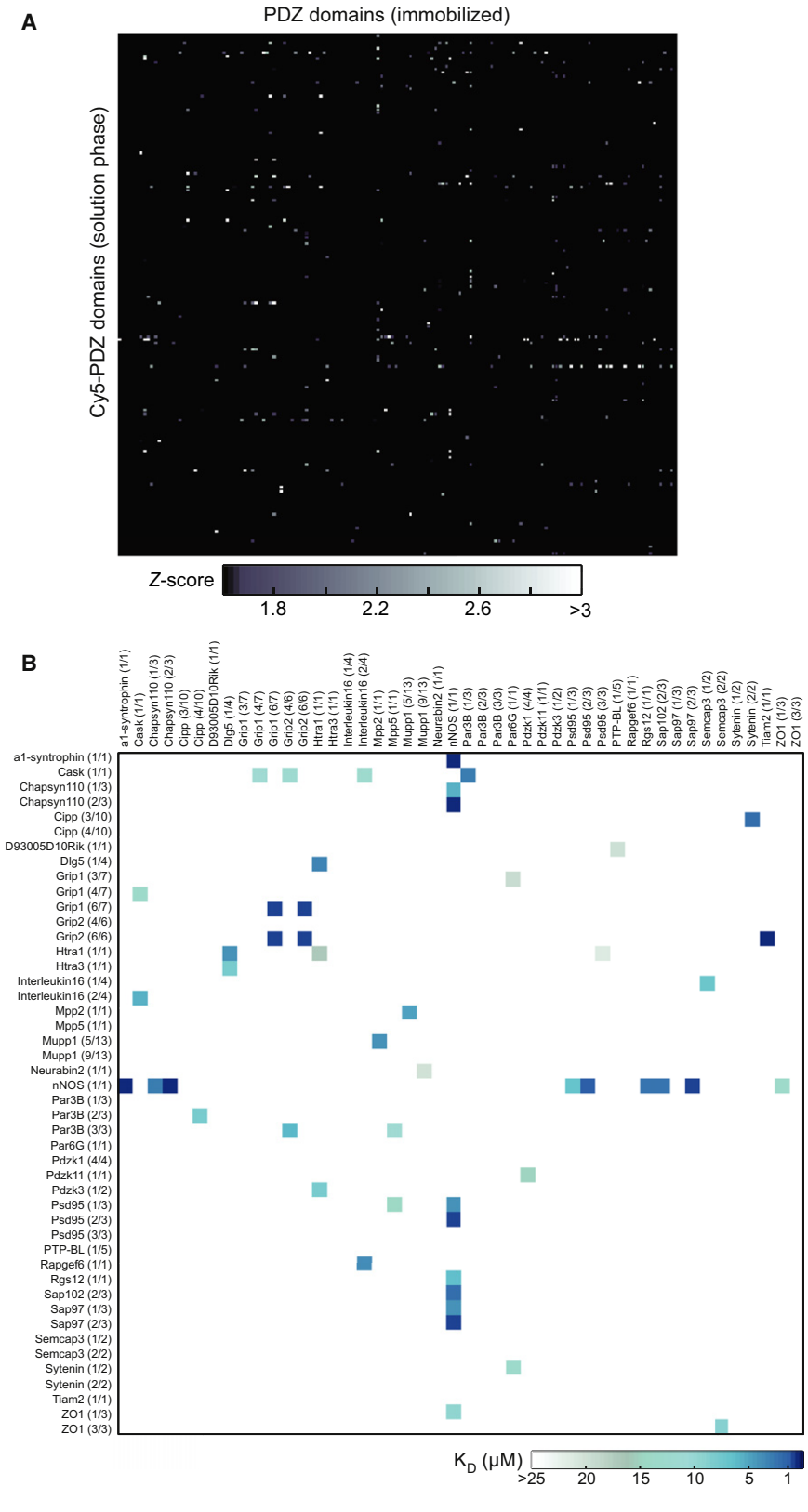

Figure 3. PDZ-PDZ Interactions

(A) PDZ-PDZ interaction matrix determined using protein microarrays. Interactions with a Z score ≥ 1.7 were designated as array-positives and are represented by colors, ranging from high Z scores (white) to low Z scores (dark blue). Array-negatives (Z score <1.7) are shown in black. Numerical values for Z scores are provided in Table S3.

(B) Quantitative PDZ-PDZ interaction matrix determined by FP. Array-positives were retested and quantified by solution-phase FP. Interactions with a K_D <25 μM are shown in colors, ranging from high affinity (dark blue) to low affinity (light gray). Negative interactions (undetectable or K_D >25 μM) are shown in white. Numerical values for all K_D values are provided in Table S4. See also Figure S1 and Table S3 and Table S4.

co-AP assays scored positive for all seven novel protein-protein interactions that we tested: GRIP2::Tiam2, CIPP::Syntenin, nNOS::SAP102, PAR3B::CASK, Rapgef6::nIL16, SAP97::nNOS, and MUPP1::MPP2 (Figure 4C). Western blots illustrating the expression of both Myc- and HA-tagged full-length proteins and of β-actin in lysates from transfected HEK293T cells are shown for all tested interactions (Figures 4A–4C).

PDZ Dimerization Is Implicated in the Assembly of Multiprotein Complexes

To probe the physiological relevance of these seven novel protein-protein interactions, we used the Gene Ontology (GO) database (http://www.geneontology.org/) to examine the cellular components (localization), biological processes, and molecular functions associated with each protein. Not surprisingly, their biological processes and molecular functions differed substantially (Table S6). However, when we examined the cellular component classifications, we observed considerable overlap for each pair of interacting proteins, providing evidence for colocalization.

Next, we used the Gene Network Central pro (GNCPro) tool (Liu et al., 2010) to determine if our novel pairs of interacting proteins were also linked through broader protein networks. GNCPro contains literature-curated information on protein-protein interactions, gene regulation, and coexpression for many mammalian proteins. When we examined the proteins involved in each novel interaction, along with the proteins directly connected to them (i.e., one level out), we found that all of the proteins in our novel interaction pairs were also connected to each other through previously established relationships (Figure 5). This lends support to their biological relevance and suggests that

Table 1. PDZ-PDZ Interactions

PDZ Domain 1	PDZ Domain 2	K_D (μM)[a]	Previously Known Interactions
a1-Syntrophin	nNOS	0.56[b,c]	Brenman et al., 1996a; Hillier et al., 1999
GRIP2 (6/6)	TIAM2	0.59	
Chapsyn-110 (2/3)	nNOS	0.66[b]	Brenman et al., 1996b
SAP97 (2/3)	nNOS	0.81	
PSD95 (2/3)	nNOS	0.92[b,c]	Brenman et al., 1996a; Tochio et al., 2000
GRIP1 (6/7)	GRIP1 (6/7)	0.98[b]	Im et al., 2003b
GRIP1 (6/7)	GRIP2 (6/6)	0.99	
GRIP2 (6/6)	GRIP2 (6/6)	1.0	
CIPP (3/10)	Syntenin (2/2)	2.2	
SAP102 (2/3)	nNOS	2.3	
nNOS	Rgs12	2.6	
CASK	PAR3B (1/3)	2.8	
nNOS (1/1)	Chapsyn-110 (1/3)	2.8	
DLG5 (1/4)	HtrA1	3.2	
Rapgef6	n-Interleukin 16 (2/4)	3.9	
SAP97 (1/3)	nNOS (1/1)	4.0	
MUPP1 (5/13)	MPP2	4.1	
PSD95 (1/3)	nNOS (1/1)	4.3	
n-Interleukin 16 (2/4)	CASK	5.8	
PAR3B (3/3)	GRIP2 (4/6)	6.1	
n-Interleukin 16 (1/4)	Semcap3 (1/2)	7.1	
Pdzk3 (1/2)	HtrA1	7.9	
HtrA3	DLG5 (1/4)	8.2	
PAR3B (2/3)	CIPP (4/10)	8.2	
ZO2 (3/3)	Semcap3 (2/2)	8.9	
ZO1 (1/3)	nNOS	9.6	
PAR3B (3/3)	MPP5	11.5	
CASK	GRIP1 (4/7)	11.7	
CASK	GRIP2 (4/6)	12.0	
Syntenin (1/2)	PAR6G	12.9	
PSD95 (1/3)	MPP5	14.2	
Pdzk11	Pdzk1 (4/4)	15.1	
HtrA1	HtrA1	17.2	
GRIP1 (3/7)	PAR6G	19.2	
D930005D10Rik	PTP-BL (1/5)	19.7	
Neurabin-2	MUPP1 (9/13)	20.2	
HtrA1	PSD95 (3/3)	21.4	

[a] K_D values were measured by FP.
[b] These interactions were previously reported.
[c] These interactions were shown to be physiologically relevant.

they either contribute to the assembly of multiprotein complexes or physically link proteins with overlapping biological functions. For example it was previously shown that nNOS interacts with PSD95, which in turn interacts with SAP102 and SAP97 (Masuko et al., 1999). Here, we find that nNOS interacts directly with both SAP102 and SAP97 through PDZ-PDZ dimerization, further strengthening this postsynaptic-signaling complex (Figure 5A). Similarly, Cask, a membrane-associated guanylate kinase, associates with the junctional proteins ZO1 and JAM2 (Kamberov et al., 2000). JAM2, in turn, interacts with Pard3 (Ebnet et al., 2003). Here, we find that Pard3 and Cask interact directly through their PDZ domains, further establishing this epithelial junctional protein network (Figure 5B). Overall, we submit that PDZ-PDZ interactions are more prevalent than previously appreciated and contribute to the formation or strengthening of multiprotein complexes.

Interestingly, PDZ-PDZ interactions appear to be substantially more selective than interactions between PDZ domains and the C termini of their target proteins. Previously, we used large-scale binding data to build a statistical model that can be used to predict interactions between mouse PDZ domains and peptide sequences (Stiffler et al., 2007). When we used this model to predict interactions on a proteome-wide level, we found that the 74 PDZ domains covered by our model recognized, on average, ~245 different proteins (Stiffler et al., 2007). In contrast the 46 PDZ domains that engage in PDZ-PDZ interactions recognize, on average, 1.7 PDZ domains (Table 1). Interestingly, in both cases the PDZ domains recognize ~1% of possible ligands (245 of 31,302 C termini in the case of PDZ-peptide interactions and 1.7 of 157 PDZ domains in the case of PDZ-PDZ interactions). However, because there are substantially fewer PDZ domains than proteins in the mammalian proteome, PDZ-PDZ interactions are much more selective than PDZ-peptide interactions. Therefore, it is possible that this noncanonical-binding mode contributes more to defining the precise composition of protein complexes than does the canonical-binding mode.

Overall, our findings support a domain-oriented approach to identifying protein-protein interactions and highlight the importance of this alternative mode of PDZ domain binding. We anticipate that the newly identified interactions highlighted by this study will serve as a useful launching point for future investigations of their biological function.

SIGNIFICANCE

Although PDZ domains typically mediate protein-protein interactions by binding to the C termini of their target proteins, it has been shown in a few instances that PDZ domain can also mediate interactions by dimerizing with another PDZ domain in either a homotypic or heterotypic fashion. However, following these early reports, very few additional interactions have been discovered, and the prevalence of this binding mode remains unclear. Here, we use a combination of protein microarrays, high-throughput solution-phase fluorescence polarization, and coaffinity purification to systematically identify PDZ-PDZ interactions across the mouse proteome. In total we identified 37 PDZ-PDZ interactions involving 46 distinct PDZ domains (~30% of all PDZ domains tested) and found that many of them mediate stable protein-protein interactions when returned to the context of their full-length proteins. The observed

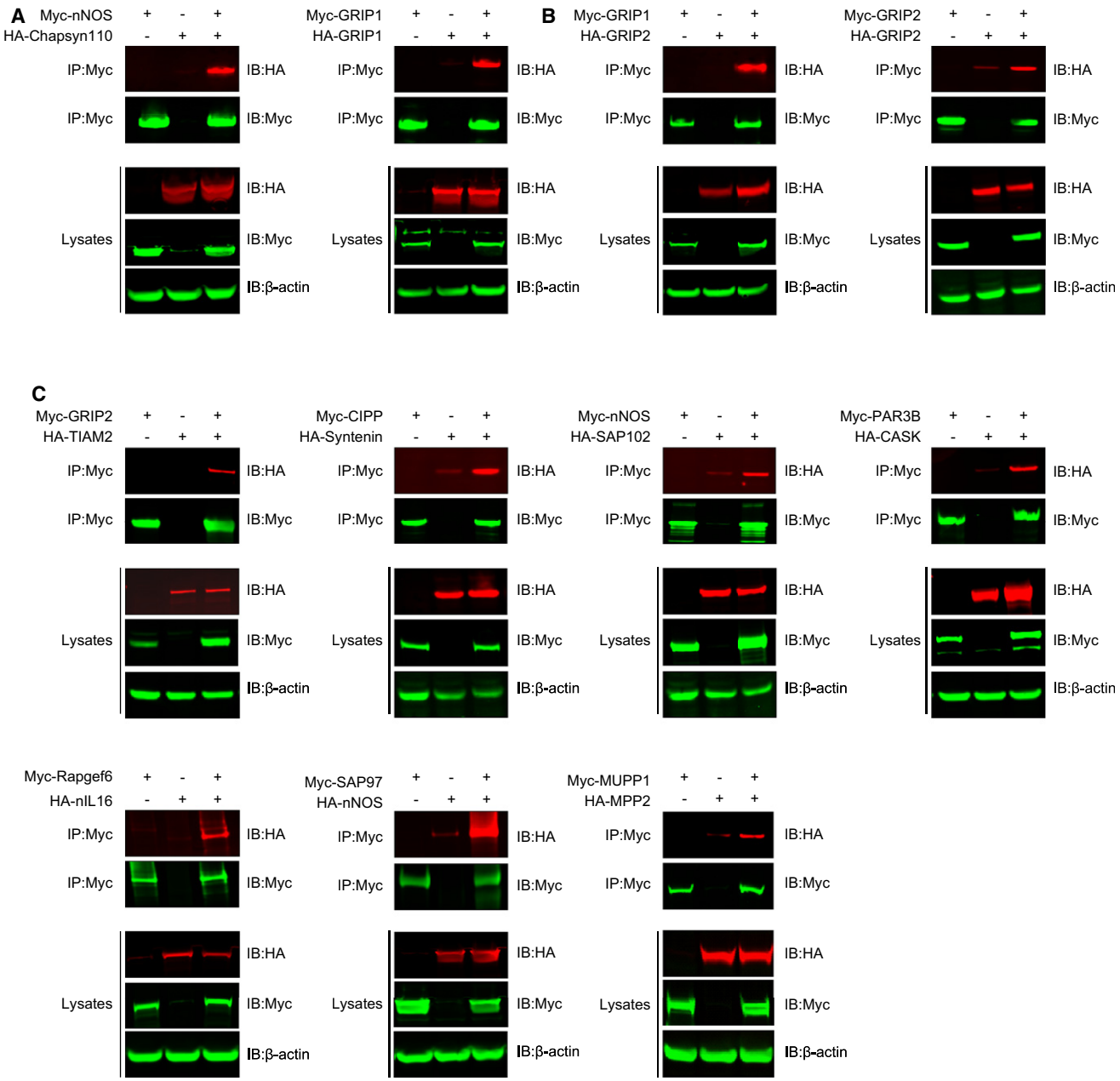

Figure 4. Biochemical Validation of PDZ-PDZ-Mediated Protein-Protein Interactions

HEK293T cells were transiently cotransfected with expression constructs encoding Myc- or HA-tagged full-length (or near full-length) PDZ domain-containing proteins. Cells were lysed 48 hr after transfection, Myc-tagged proteins were immunoprecipitated, and Myc- or HA-tagged proteins were detected by immunoblotting.

(A) Western blots showing the previously reported interaction between nNOS and Chapsyn110 (Brenman et al., 1996b) and the previously reported homodimerization of Grip1 (Im et al., 2003b).

(B) Western blots showing interaction between Grip1 and Grip2 and homodimerization of Grip2.

(C) Western blots showing association of GRIP2 with Tiam2, CIPP with Syntenin, nNOS with SAP102, PAR3B with CASK, Rapgef6 with nIL16, SAP97 with nNOS, and MUPP1 with MPP2. Lysates immunoblotted with anti-Myc, anti-HA, and anti-β-actin are shown as transfection and loading controls.

See also Table S5.

prevalence of PDZ domain dimerization shows that this binding mode occurs at a higher frequency than previously appreciated and suggests that many PDZ domains evolved to guide the assembly of multiprotein complexes. On a broader level this study shows that focusing on families of protein-interaction modules provides a viable way to segment the challenging task of identifying protein-protein interactions on a proteome-wide scale.

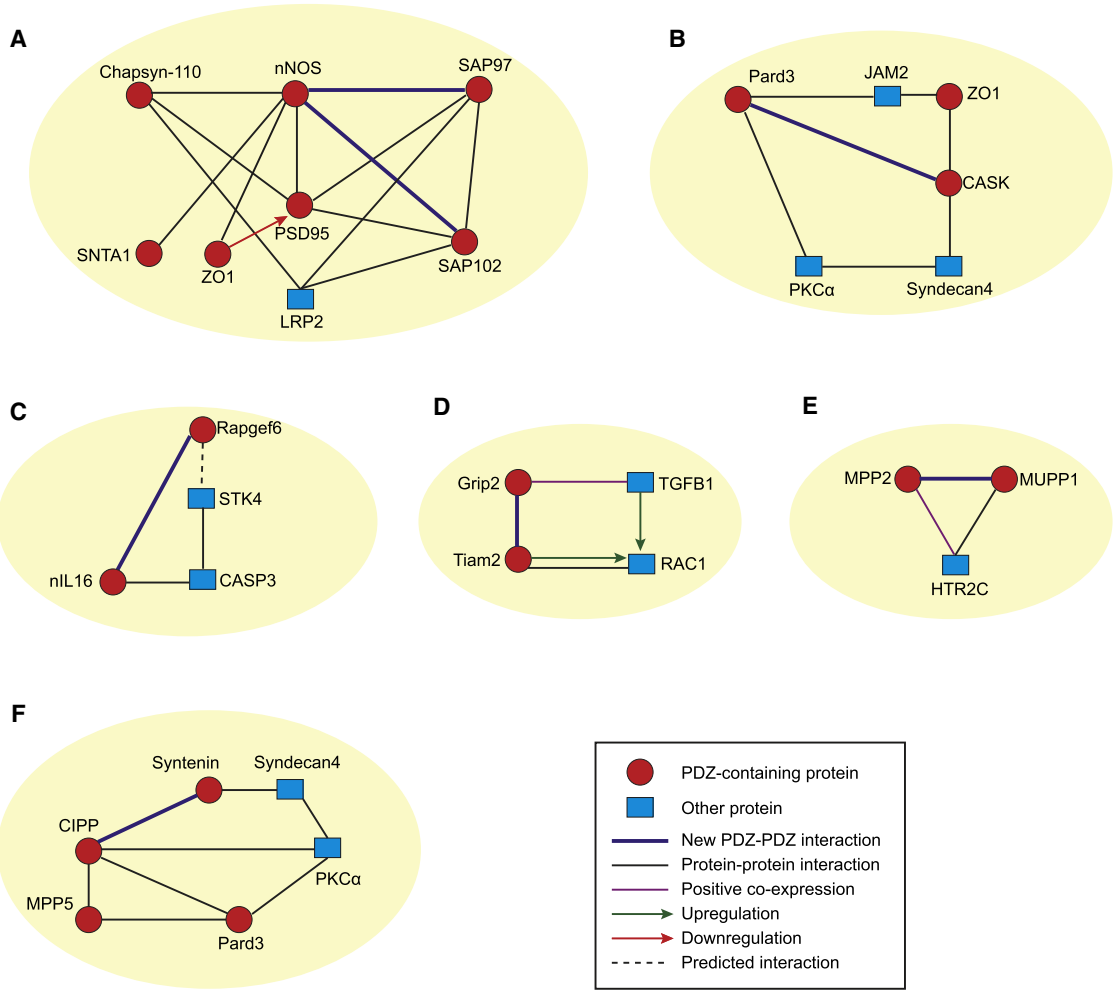

Figure 5. Protein-Interaction Networks of PDZ Domain-Containing Proteins

Protein-interaction networks were constructed for each of the seven new, biochemically confirmed protein-protein interactions using the GNCPro tool. Only proteins that had direct connections to the PDZ domain-containing proteins were included in each graph. Networks include: (A) nNOS::SAP102 and nNOS::SAP97; (B) Pard3::CASK; (C) nIL16::Rapgef6; (D) Grip2::Tiam2; (E) MPP2::MUPP1; and (F) CIPP::Syntenin. See also Table S6.

EXPERIMENTAL PROCEDURES

Cloning of PDZ domains and production and purification of recombinant proteins were performed as previously described (Chen et al., 2008; Stiffler et al., 2006, 2007).

Fluorophore Labeling of PDZ domains

N-hydroxy succinimidyl esters of cyanine-3 (Cy3) and cyanine-5 (Cy5) fluorescent dyes were obtained as a dry powder (GE Healthcare, Pittsburgh). Each vial of dye was dissolved in 100 μl of Buffer A (100 mM KCl, 10 mM NaH_2PO_4/Na_2HPO_4 [pH 7.4]). A total of 20 μl of this dye solution was added to 200 μl of a room temperature solution of 80 μM PDZ domain in Buffer A. After 30 min at room temperature, the protein/dye solution was diluted to 1 ml using Buffer A. Immediately after dilution, unreacted dye was separated from dye-labeled PDZ domain using NAP10 gel permeation chromatographic columns (GE Healthcare). Protein concentration and protein-to-dye ratios were determined on the basis of absorbance at 280 and 552 nm (Cy3) or 650 nm (Cy5). Labeled proteins were aliquoted and stored at −80°C.

Manufacturing and Processing of Protein Microarrays

Purified recombinant PDZ domains, doped with 100 nM Cy3-labeled BSA, were spotted at a concentration of 40 μM onto 112.5 × 74.5 × 1 mm aldehyde-displaying glass substrates (Erie Scientific Co., Portsmouth, NH) using a BioChip Arrayer (PerkinElmer, Boston). A total of 96 identical microarrays were printed in an 8 × 12 pattern on the glass plates, with a pitch of 9 mm. Each microarray consisted of a 20 × 20 pattern of spots, with a center-to-center spacing of 250 μm. Proteins were spotted in quadruplicate. Following an overnight incubation the glass was attached to the bottom of a bottomless 96-well microtiter plate (Greiner Bio-One, Kremsmünster, Austria) using an intervening silicone gasket (Grace Bio-Labs, Bend, OR). Immediately before use, the plates were quenched with Buffer A containing 1% BSA (w/v) for 1 hr at room temperature, followed by incubation in Buffer A containing 1% BSA (w/v) and 50 mM glycine. The arrays were rinsed briefly in Buffer A containing 0.1% Tween 20 (v/v) and probed with a 0.1 μM concentration of Cy5-labeled PDZ domain dissolved in Buffer B (100 mM KCl, 1% BSA [w/v], 0.1% Tween 20 [v/v], 10 mM Na_2HPO_4/NaH_2PO_4 [pH7.4]). Following a 1 hr incubation at room temperature, the peptide solution was removed, and the arrays were washed with 300 μl of Buffer A containing 0.1% Tween 20 (v/v). The arrays were rinsed twice with 300 μl of ddH_2O and spun upside down in a centrifuge for 60 s to remove residual water.

Scanning and Analysis of Protein Microarrays

PDZ microarrays were scanned at 10 μm resolution using a Tecan LS400 microarray scanner (Tecan, Männedorf, Switzerland). Cy5 fluorescence was

imaged using a 633 nm laser, and Cy3 fluorescence was imaged using a 543 nm laser. Images were analyzed using Array-Pro image analysis software (Media Cybernetics, Bethesda, MD) and MATLAB (MathWorks, Natick, MA). Microarray spots were identified on the basis of the Cy3 image, and the mean Cy5 fluorescence of each protein was calculated from the four replicate spots. Z-score values were determined separately using the mean of all data points from each Cy5 PDZ domain probe.

Site-Directed Mutagenesis of PDZ Domain C Termini

The coding region for the three C-terminal residues of the PDZ domain was changed to three consecutive glycines using the QuikChange Site-Directed Mutagenesis Kit (Stratagene, La Jolla, CA). Primers were designed using an online design tool (Stratagene) and ordered as complimentary pairs (Invitrogen, Carlsbad, CA). Mutant clones were verified by DNA sequencing.

Fluorescence Polarization

Purified recombinant PDZ domains were introduced into separate wells in column 1 of a 96-well microtiter plate (2 ml/well) at a concentration of 25 μM. The remaining wells of the plate were filled with Buffer A supplemented with 2.5 mM dithiothreitol (DTT), and 2-fold serial dilutions of each domain were prepared across each row. DTT was added to all wells in column 1, resulting in a 1.25 mM DTT concentration across all wells. Cy3-labeled PDZ domains were diluted to a concentration of 100 nM in Buffer A. A 10 μl portion of Cy3-labeled PDZ probe solution was then transferred to alternating wells of a row in a 384-well microtiter plate using a multichannel pipette. A 40 μl portion of a PDZ domain dilution series was then transferred to alternating wells of the 384-well plate using a multichannel pipette, resulting in two separate PDZ/Cy3-PDZ titrations per row and 32 titrations per 384-well plate. Plates were incubated at room temperature for 12 hr. After spinning the plates down, Cy3 fluorescence was detected using an Analyst AD fluorescence plate reader (Molecular Devices, Sunnyvale, CA), with excitation at 525 nm and emission at 590 nm. FP, in millipolarization units (mP), was defined as $10^3 \times (I^{\parallel} - I^{\perp})/(I^{\parallel} + I^{\perp})$, where $I^{\parallel}$ and $I^{\perp}$ are the fluorescence intensities parallel and perpendicular to the plane of incident light, respectively. Data for each PDZ/Cy3-PDZ interaction were fit to Equation 1 using a general curve-fitting algorithm (MATLAB). An interaction was scored as "positive" if it fit well to Equation 1 ($R^2 \geq 0.95$), had a $K_D \leq 25$ μM, and had a high signal ($FP - FP_0 \geq 15$ mP at 20 μM PDZ domain).

Mammalian Expression Constructs

Plasmids containing full-length or nearly full-length ORFs for PDZ domain-containing proteins were obtained commercially (Thermo Scientific-Open Biosystems, Huntsville, AL). All ORFs were subcloned into the vector pENTR/D-TOPO by topoisomerase I-mediated directional cloning (Invitrogen). The coding region for each construct was transferred into the mammalian expression vectors pCMV-MYC and pCMV-HA (Clontech, Mountain View, CA) via λ-recombinase mediated directional subcloning. Each clone was verified by DNA sequencing.

Cell Lines and Reagents

HEK293T and HeLa cells were obtained from American Type Culture Collection (ATCC, Rockville, MD) and maintained in Dulbecco's Modified Eagle's Medium (DMEM) supplemented with 10% (v/v) fetal bovine serum (FBS), 2 mM glutamine, 100 IU/ml penicillin, and 100 μg/ml streptomycin. Primary antibodies were obtained from the following sources: mouse anti-MYC (Cell Signaling Technology, Danvers, MA; catalog #2276); rabbit anti-HA (Cell Signaling Technology; catalog #3724); and mouse anti-β-actin (Sigma-Aldrich, Inc., St. Louis; catalog #A1978).

Transfections and Coaffinity Purifications

For cotransfection experiments, cells were grown to 75% confluency in 100 mm dishes. A total of 3 μg of each tagged pCMV plasmid was transfected into HEK293T cells using Lipofectamine 2000 according to the manufacturer's instructions (Invitrogen). After 12 hr, the media were aspirated, and new media were added. Two days after transfections, the cells were washed twice with cold phosphate-buffered saline, harvested, and lysed with 500 μl of lysis buffer (Cell Signaling Technology; catalog #9803) supplemented with 1 mM phenylmethylsulfonyl fluoride and a cocktail of protease inhibitors (Roche Applied Science, Indianapolis, IN; 1 tablet per 10 ml) on ice for 30 min. Whole-cell lysates were cleared by centrifugation at 20,000 × g for 10 min at 4°C.

For co-AP experiments, lysates were incubated with a 1:50 dilution of the appropriate primary antibody with agitation for 2 hr at 4°C, mixed with a 1:10 dilution of Protein A/G PLUS-Agarose (Santa Cruz Biotechnology; catalog #SC-2003), and incubated on ice for 1 hr with agitation. Immunoprecipitates were pelleted, washed, and resuspended in NuPAGE LDS Sample Buffer (Invitrogen; catalog #NP0007), and subjected to immunoblotting.

Immunoblotting

Prior to immunoblotting, lysates were boiled in NuPAGE LDS Sample Buffer and loaded onto NuPAGE Novex 4%–12% Bis-Tris 1.0 mm, 15-well precast gels (Invitrogen; catalog #NP0323). All solutions and procedures were performed according to manufacturer instructions. After separation by electrophoresis, the proteins were transferred to nitrocellulose, and the membranes were blocked with 5% nonfat dry milk (w/v) in phosphate-buffered saline. Membranes were probed using a mouse-anti-MYC antibody (Cell Signaling Technology), a rabbit-anti-HA antibody (Cell Signaling Technology), and/or a mouse-anti-β-actin antibody (Sigma-Aldrich). Bands were detected with IRDye 680-labeled goat-anti-rabbit IgG and IRDye 800CW-labeled goat-anti-mouse (LI-COR Biosciences, Lincoln, NE) and imaged using an Odyssey Infrared Imaging System (LI-COR Biosciences).

SUPPLEMENTAL INFORMATION

Supplemental Information includes one figure and six tables and can be found with this article online at doi:10.1016/j.chembiol.2011.06.013.

ACKNOWLEDGMENTS

This study was supported by an award from the Arnold and Mabel Beckman Foundation and by a grant from the National Institutes of Health (R01 GM072872). T.S.G. is a Human Frontier Science Program Fellow, and E.S.K. is the recipient of a National Science Foundation Graduate Fellowship. G.M. is a founder, employee, and shareholder of Merrimack Pharmaceuticals; a founder and shareholder of Makoto Life Sciences; and a scientific advisory board member of Aushon Biosystems. R.B. and V.P.G. are employees and shareholders of Merrimack Pharmaceuticals.

Received: March 22, 2011
Revised: May 20, 2011
Accepted: June 3, 2011
Published: September 22, 2011

REFERENCES

Bilder, D. (2001). PDZ proteins and polarity: functions from the fly. Trends Genet. *17*, 511–519.

Brenman, J.E., Chao, D.S., Gee, S.H., McGee, A.W., Craven, S.E., Santillano, D.R., Wu, Z., Huang, F., Xia, H., Peters, M.F., et al. (1996a). Interaction of nitric oxide synthase with the postsynaptic density protein PSD-95 and alpha1-syntrophin mediated by PDZ domains. Cell *84*, 757–767.

Brenman, J.E., Christopherson, K.S., Craven, S.E., McGee, A.W., and Bredt, D.S. (1996b). Cloning and characterization of postsynaptic density 93, a nitric oxide synthase interacting protein. J. Neurosci. *16*, 7407–7415.

Chen, J.R., Chang, B.H., Allen, J.E., Stiffler, M.A., and MacBeath, G. (2008). Predicting PDZ domain-peptide interactions from primary sequences. Nat. Biotechnol. *26*, 1041–1045.

Cho, K.O., Hunt, C.A., and Kennedy, M.B. (1992). The rat brain postsynaptic density fraction contains a homolog of the *Drosophila* discs-large tumor suppressor protein. Neuron *9*, 929–942.

Doyle, D.A., Lee, A., Lewis, J., Kim, E., Sheng, M., and MacKinnon, R. (1996). Crystal structures of a complexed and peptide-free membrane protein-binding domain: molecular basis of peptide recognition by PDZ. Cell *85*, 1067–1076.

Ebnet, K., Aurrand-Lions, M., Kuhn, A., Kiefer, F., Butz, S., Zander, K., Meyer zu Brickwedde, M.K., Suzuki, A., Imhof, B.A., and Vestweber, D. (2003). The junctional adhesion molecule (JAM) family members JAM-2 and JAM-3 associate with the cell polarity protein PAR-3: a possible role for JAMs in endothelial cell polarity. J. Cell Sci. *116*, 3879–3891.

Ernst, A., Sazinsky, S.L., Hui, S., Currell, B., Dharsee, M., Seshagiri, S., Bader, G.D., and Sidhu, S.S. (2009). Rapid evolution of functional complexity in a domain family. Sci. Signal. *2*, ra50.

Fouassier, L., Yun, C.C., Fitz, J.G., and Doctor, R.B. (2000). Evidence for ezrin-radixin- moesin-binding phosphoprotein 50 (EBP50) self-association through PDZ-PDZ interactions. J. Biol. Chem. *275*, 25039–25045.

Garner, C.C., Nash, J., and Huganir, R.L. (2000). PDZ domains in synapse assembly and signalling. Trends Cell Biol. *10*, 274–280.

Harris, B.Z., and Lim, W.A. (2001). Mechanism and role of PDZ domains in signaling complex assembly. J. Cell Sci. *114*, 3219–3231.

Harris, B.Z., Hillier, B.J., and Lim, W.A. (2001). Energetic determinants of internal motif recognition by PDZ domains. Biochemistry *40*, 5921–5930.

Hillier, B.J., Christopherson, K.S., Prehoda, K.E., Bredt, D.S., and Lim, W.A. (1999). Unexpected modes of PDZ domain scaffolding revealed by structure of nNOS-syntrophin complex. Science *284*, 812–815.

Im, Y.J., Lee, J.H., Park, S.H., Park, S.J., Rho, S.H., Kang, G.B., Kim, E., and Eom, S.H. (2003a). Crystal structure of the Shank PDZ-ligand complex reveals a class I PDZ interaction and a novel PDZ-PDZ dimerization. J. Biol. Chem. *278*, 48099–48104.

Im, Y.J., Park, S.H., Rho, S.H., Lee, J.H., Kang, G.B., Sheng, M., Kim, E., and Eom, S.H. (2003b). Crystal structure of GRIP1 PDZ6-peptide complex reveals the structural basis for class II PDZ target recognition and PDZ domain-mediated multimerization. J. Biol. Chem. *278*, 8501–8507.

Jameson, D.M., and Seifried, S.E. (1999). Quantification of protein-protein interactions using fluorescence polarization. Methods *19*, 222–233.

Kamberov, E., Makarova, O., Roh, M., Liu, A., Karnak, D., Straight, S., and Margolis, B. (2000). Molecular cloning and characterization of Pals, proteins associated with mLin-7. J. Biol. Chem. *275*, 11425–11431.

Liu, G.G., Fong, E., and Zeng, X. (2010). GNCPro: navigate human genes and relationships through net-walking. Adv. Exp. Med. Biol. *680*, 253–259.

Masuko, N., Makino, K., Kuwahara, H., Fukunaga, K., Sudo, T., Araki, N., Yamamoto, H., Yamada, Y., Miyamoto, E., and Saya, H. (1999). Interaction of NE-dlg/SAP102, a neuronal and endocrine tissue-specific membrane-associated guanylate kinase protein, with calmodulin and PSD-95/SAP90. A possible regulatory role in molecular clustering at synaptic sites. J. Biol. Chem. *274*, 5782–5790.

Maudsley, S., Zamah, A.M., Rahman, N., Blitzer, J.T., Luttrell, L.M., Lefkowitz, R.J., and Hall, R.A. (2000). Platelet-derived growth factor receptor association with Na(+)/H(+) exchanger regulatory factor potentiates receptor activity. Mol. Cell. Biol. *20*, 8352–8363.

Nourry, C., Grant, S.G., and Borg, J.P. (2003). PDZ domain proteins: plug and play! Sci. STKE *2003*, RE7.

Sheng, M., and Sala, C. (2001). PDZ domains and the organization of supramolecular complexes. Annu. Rev. Neurosci. *24*, 1–29.

Songyang, Z., Fanning, A.S., Fu, C., Xu, J., Marfatia, S.M., Chishti, A.H., Crompton, A., Chan, A.C., Anderson, J.M., and Cantley, L.C. (1997). Recognition of unique carboxyl-terminal motifs by distinct PDZ domains. Science *275*, 73–77.

Srivastava, S., Osten, P., Vilim, F.S., Khatri, L., Inman, G., States, B., Daly, C., DeSouza, S., Abagyan, R., Valtschanoff, J.G., et al. (1998). Novel anchorage of GluR2/3 to the postsynaptic density by the AMPA receptor-binding protein ABP. Neuron *21*, 581–591.

Stiffler, M.A., Grantcharova, V.P., Sevecka, M., and MacBeath, G. (2006). Uncovering quantitative protein interaction networks for mouse PDZ domains using protein microarrays. J. Am. Chem. Soc. *128*, 5913–5922.

Stiffler, M.A., Chen, J.R., Grantcharova, V.P., Lei, Y., Fuchs, D., Allen, J.E., Zaslavskaia, L.A., and MacBeath, G. (2007). PDZ domain binding selectivity is optimized across the mouse proteome. Science *317*, 364–369.

Tochio, H., Mok, Y.K., Zhang, Q., Kan, H.M., Bredt, D.S., and Zhang, M. (2000). Formation of nNOS/PSD-95 PDZ dimer requires a preformed beta-finger structure from the nNOS PDZ domain. J. Mol. Biol. *303*, 359–370.

Utepbergenov, D.I., Fanning, A.S., and Anderson, J.M. (2006). Dimerization of the scaffolding protein ZO-1 through the second PDZ domain. J. Biol. Chem. *281*, 24671–24677.

Woods, D.F., and Bryant, P.J. (1993). ZO-1, DlgA and PSD-95/SAP90: homologous proteins in tight, septate and synaptic cell junctions. Mech. Dev. *44*, 85–89.

Xu, X.Z.S., Choudhury, A., Li, X., and Montell, C. (1998). Coordination of an array of signaling proteins through homo- and heteromeric interactions between PDZ domains and target proteins. J. Cell Biol. *142*, 545–555.

Yan, Y., and Marriott, G. (2003). Analysis of protein interactions using fluorescence technologies. Curr. Opin. Chem. Biol. *7*, 635–640.

